# Durham Research Online

---

**Deposited in DRO:**

22 August 2014

**Version of attached file:**

Published Version

**Peer-review status of attached file:**

Peer-reviewed

**Citation for published item:**

Sawangwit, U. and Shanks, T. and Croom, S.M. and Drinkwater, M.J. and Fine, S. and Parkinson, D. and Ross, N.P. (2012) 'Measuring BAO and non-Gaussianity via QSO clustering.', Monthly notices of the Royal Astronomical Society., 420 (3). pp. 1916-1925.

**Further information on publisher's website:**

http://dx.doi.org/10.1111/j.1365-2966.2011.19848.x

**Additional information:**

# Measuring BAO and non-Gaussianity via QSO clustering

U. Sawangwit,[1][*] T. Shanks,[1] S. M. Croom,[2] M. J. Drinkwater,[3] S. Fine,[1] D. Parkinson[3] and Nicholas P. Ross[4]

[1]*Department of Physics, Durham University, South Road, Durham DH1 3LE*
[2]*Sydney Institute for Astronomy, School of Physics, University of Sydney, NSW 2006, Australia*
[3]*School of Mathematics & Physics, The University of Queensland, Brisbane, QLD 4072, Australia*
[4]*Lawrence Berkeley National Laboratory, One Cyclotron Road, Berkeley, CA 94720, USA*

**ABSTRACT**

Our goals are (i) to search for BAO and large-scale structure in current quasi-stellar object (QSO) survey data and (ii) to use these and simulation/forecast results to assess the science case for a new, $\gtrsim$10 times larger, QSO survey. We first combine the Sloan Digital Sky Survey (SDSS), 2dF QSO Redshift Survey (2QZ) and 2dF-SDSS LRG and QSO (2SLAQ) surveys to form a survey of $\approx$60 000 QSOs. We find a hint of a peak in the QSO two-point correlation function, $\xi(s)$, at the same scale ($\approx$105 $h^{-1}$ Mpc) as detected by Eisenstein et al. in their sample of Data Release 5 (DR5) Luminous Red Galaxies (LRGs) but only at low statistical significance. We then compare these data with QSO mock catalogues from the Hubble Volume $N$-body light-cone simulation used by Hoyle et al. and find that both routes give statistical error estimates that are consistent at $\approx$100 $h^{-1}$ Mpc scales. Mock catalogues are then used to estimate the nominal survey size needed for a 3–4$\sigma$ detection of the Baryon Acoustic Oscillations (BAO) peak. We find that a redshift survey of $\approx$250 000 $z < 2.2$ QSOs is required over $\approx$3000 deg$^2$. This is further confirmed by static lognormal simulations where the BAO are clearly detectable in the QSO power spectrum and correlation function. The nominal survey would on its own produce the first detection of, for example, discontinuous dark energy evolution in the so far uncharted $1 < z < 2.2$ redshift range. We further find that a survey with $\approx$50 per cent higher QSO sky densities and 50 per cent bigger area will give an $\approx$6$\sigma$ BAO detection, leading to an error $\approx$60 per cent of the size of the BOSS error on the dark energy evolution parameter, $w_a$.

Another important aim of a QSO survey is to place new limits on primordial non-Gaussianity at large scales. In particular, it is important to test tentative evidence we have found for the evolution of the linear form of the combined SDSS+2QZ+2SLAQ QSO $\xi(s)$ at $z \approx 1.6$, which may be caused by the existence of non-Gaussian clustering features at high redshift. Such a QSO survey will also determine the gravitational growth rate at $z \approx 1.6$ via redshift-space distortions, allow lensing tomography via QSO magnification bias while also measuring the exact luminosity dependence of small-scale QSO clustering.

**Key words:** quasars: general – cosmology: observations – dark energy – distance scale – inflation – large-scale structure of Universe.

## 1 INTRODUCTION

Quasi-stellar objects (QSOs) have been used as tracers of large-scale structure for many years now. The first measurements were made by Osmer (1981), then with the arrival of high-multiplex fibre systems, the subject advanced rapidly (e.g. Boyle, Shanks & Peterson 1988; Croom et al. 2005; da Ângela et al. 2008; Ross et al.

2009 and references therein). Their clustering at small scales as measured by the correlation function is known to be consistent with the usual $\gamma = -1.8$ power-law form for galaxies. The amplitude is comparable to galaxies at low redshifts and remains reasonably constant with redshift. At larger scales the power spectrum has been measured to be reasonably consistent with the standard $\Lambda$cold dark matter ($\Lambda$CDM) cosmological model (e.g. Hoyle et al. 2002; Outram et al. 2003).

Here, we have combined the largest, spectroscopically confirmed, QSO surveys from fibre spectrographs including 2QZ (Croom et al.

2004), 2SLAQ (Croom et al. 2009) and SDSS DR5 (Schneider et al. 2007) to form a redshift survey comprising some $\approx 60\,000$ QSOs. We have already found in these data sets that the small-scale clustering of QSOs is remarkably independent of QSO luminosity at fixed redshift (Shanks et al. 2011).

In this paper, we first use the above combined survey to estimate the large-scale QSO correlation function and search for the BAO feature. We then outline our initial motivation for an extended QSO redshift survey using the 'effective survey volume' as a measure of clustering 'grasp'. We then make an empirical test of the errors on the QSO correlation function at $\approx 100\,h^{-1}$ Mpc scales using both the data and mock QSO catalogues from the Hubble Volume *N*-body simulation. These routes allow a first estimate of the survey size needed for a significant BAO detection. We particularly focus on surveys that could be made with Two-degree Field (2dF) (Lewis et al. 2002) and AAOmega (Smith et al. 2004) at the Anglo-Australian Telescope [AAT; cf. the results of Wang et al. 2009 for QSO surveys with The Large Sky Area Multi-Object Fiber Spectroscopic Telescope (LAMOST)]. We then use static lognormal simulations to test further BAO detectability and use Fisher matrix and Markov Chain Monte Carlo (MCMC) methods to test a QSO survey's competitiveness against other routes to the BAO scale and the evolution of $w$. Finally, we look at the prospects of detecting evidence for non-Gaussian clustering at large scales via a QSO survey, in particular focusing on the possibility that the current QSO surveys show evidence for evolution in the linear regime of clustering, which might represent evidence for non-Gaussianity, if confirmed in a larger survey.

## 2 QSO CLUSTERING DATA

We start by making a study of the results from current QSO surveys (a) to see if the BAO peak can be detected in the correlation function and (b) to measure the errors to base an empirical estimate of the new survey size needed for an accurate BAO measurement. This survey size estimate will then be compared to those from simulations to determine the best QSO survey strategy in terms of area and magnitude limit.

### 2.1 SDSS, 2QZ and 2SLAQ surveys

Previously, Croom et al. (2005) used the 2QZ survey to estimate the QSO correlation function and its dependence on redshift and luminosity. This survey contained $\approx 22\,655$ QSOs in two $\approx 375\,\deg^2$ NGC + SGC strips. The magnitude limit was $18.25 < b_J < 20.85$ and the resulting QSO sky density was $31\,\deg^{-2}$. Croom et al. (2005) measured $s_0 = 5.4^{+0.42}_{-0.48}\,h^{-1}$ Mpc and $\gamma = 1.2 \pm 0.1$ at $1 < s < 25\,h^{-1}$ Mpc for the amplitude and slope of the *z*-space correlation function, $\xi(s)$.

da Ângela et al. (2008) then used the 2SLAQ survey of 9418 QSOs based on SDSS imaging to test the luminosity dependence of the QSO clustering. The magnitude limit was $20.5 < g_{AB}(\approx b_J) < 21.85$ and the resulting QSO sky density was $\approx 45\,\deg^{-2}$, including the 2dF QSOs where the two surveys overlapped, in a total area of $\approx 200\,\deg^2$. da Ângela et al. (2008) found a $\xi(s)$ amplitude and slope similar to that for 2QZ.

Most recently, Ross et al. (2009) have analysed the clustering of 30239 QSOs in the 4013 $\deg^2$ SDSS DR5 survey to $i_{AB} = 19.1$. This gives a QSO sky density of $7.5\,\deg^{-2}$ in the uniform sample where Ross et al. (2009) measured $s_0 = 5.95 \pm 0.45\,h^{-1}$ Mpc and $\gamma = 1.16^{+0.11}_{-0.16}$ in the $1 < s < 25\,h^{-1}$ Mpc range.

### 2.2 Large-scale clustering comparison

Here, the clustering analysis has been re-done to use consistent bins at comoving separations corresponding to BAO scales in the 2QZ, 2SLAQ and SDSS-DR5 spectroscopic QSO samples. The data and random catalogues are the same as those used in the analyses of da Ângela et al. (2008) and Ross et al. (2009) for 2QZ+2SLAQ and SDSS-DR5, respectively. We used the 'UNIFORM' sample with $0.3 \leq z \leq 2.2$ of Ross et al. (2009) which contains 30 239 QSOs over 4013 $\deg^2$. The 2QZ+2SLAQ sample contains 28 790 $0.3 < z < 2.9$ QSOs and its small- and intermediate-scale clustering analyses have been performed by da Ângela et al. (2008) [see also Croom et al. (2005) for the 2QZ-only clustering analysis]. We perform a new clustering analysis by counting pairs at separation, *s*, independently for the SDSS and 2QZ+2SLAQ samples. The data–random (*DR*) and random–random (*RR*) pairs for each sample are normalized by $N_{rd}$ and $N_{rd}^2$, respectively, where $N_{rd}$ is the ratio between numbers of randoms and data ($\approx 20$ for the 2QZ+2SLAQ and $\approx 30$ for the SDSS samples). The Landy & Szalay (1993) estimator is then used to determine the $\xi(s)$ from the summed pairs over the different samples. Note that the results are in good agreement with those using the Hamilton (1993) estimator.

In Fig. 1 we then compare the large-scale clustering results from the three surveys directly with each other using the redshift-space correlation function, $\xi(s)$. The cosmology assumed in all cases is $\Omega_\Lambda = 0.7$, $\Omega_m = 0.3$. Fitting the $\xi(s)$ results consistently in the $1 < s < 30\,h^{-1}$ Mpc range, Shanks et al. (2011) fitted real-space correlation function scalelengths, $r_0$, assuming power-law slope, $\gamma = 1.8$, infall parameter, $\beta = 0.4$, and line-of-sight pairwise velocity dispersion $\langle w^2 \rangle^{1/2} = 750\,\mathrm{km\,s^{-1}}$. These authors found agreement at the $1.4\sigma$ significance level in these results with SDSS giving $r_0 = 6.30 \pm 0.3\,h^{-1}$ Mpc, 2QZ giving $r_0 = 5.75 \pm 0.25\,h^{-1}$ Mpc and 2SLAQ giving $r_0 = 5.70 \pm 0.35\,h^{-1}$ Mpc. The best overall fit is $r_0 = 5.90 \pm 0.14\,h^{-1}$ Mpc. Thus the small-scale results suggest that it is reasonable to combine these three surveys and the $\xi(s)$ result at large scales is also shown in Fig. 1. The data are compared to a Lambda-Cold Dark Matter (LCDM) model and a 'wiggle-free'
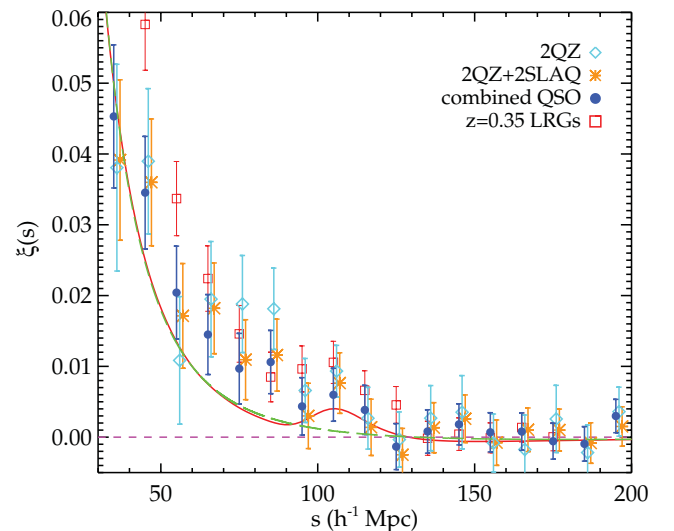


**Figure 1.** The large-scale redshift-space correlation function results from the 2QZ, the 2QZ+2SLAQ and the combined SDSS DR5+2QZ+2SLAQ QSO surveys. The errors are empirically scaled by the average (1.2 times) ratio of jack-knife to Poisson errors in this separation range. The results are compared to $\Lambda$CDM (red solid) and no-wiggle (green dashed) models and also the $z = 0.35$ LRG result of Eisenstein et al. (2005).

version of the model (Eisenstein & Hu 1998). These models are normalized to match the data at $s = 10 - 30\,h^{-1}$ Mpc (see Fig. 9). The errors are based on Poisson errors calibrated by jack-knife errors in all three cases. Generally, the SDSS has the biggest errors, particularly at the smaller scales. This is because of its relatively low sky density. This means that at $\approx 100\,h^{-1}$ Mpc the 2QZ (and 2SLAQ) surveys dominate the statistics at the predicted BAO scale. The 2QZ survey error is $\approx 2$ times smaller than the SDSS error and 1.8 times smaller than the 2SLAQ error. The blue filled circles then represent the overall 2QZ+2SLAQ+SDSS result, produced by simply adding the QSO–QSO and QSO–random pairs across the surveys. The resulting error is $\approx 2$ times larger than the error from the SDSS LRG sample of Eisenstein et al. (2005). We see that there is some hint of a detection at $105\,h^{-1}$ Mpc but there is a similarly sized feature at $\approx 85\,h^{-1}$ Mpc. Clearly while the data appear promising in terms of detecting the BAO feature, a larger sample size is needed and in Section 5 we will translate these empirical errors into a required survey size to measure the BAO scale. We shall also compare with the errors predicted by simulations and use these to optimize the properties of a new QSO redshift survey for large-scale clustering.

## 3 QSO SURVEY EFFECTIVE VOLUME

We next estimate the efficiency of future QSO clustering surveys via their effective volume ($V_{eff}$). Although QSO sky densities are lower than for galaxy surveys, their clustering amplitude is relatively high, the exposure time required to establish redshifts is generally quite short, contamination rates are increasingly low and the volumes probed are very large. Moreover, the low QSO sky density can be viewed as an advantage in that it may well match the fibre density currently available from instruments like AAT 2dF.

A rough measure of a survey's capability for power spectrum or two-point correlation function analysis, the effective volume is defined by Eisenstein et al. (2005) and represents the survey volume that has a high enough QSO density for the shot noise to lie below the amplitude of a spatial power spectrum feature such as a BAO oscillation scale. The power spectrum or correlation function error at a particular scale then is proportional to $V_{eff}^{-1/2}$. In Fig. 2 we have calculated the effective volume for QSO surveys assuming the SDSS DR5 QSO $n(z)$ in the redshift range $0.5 < z < 2.2$ (see also fig. 2 of Wang et al. 2009). We have chosen a nominal survey area of $3000\,\mathrm{deg}^2$; effective volumes of other survey areas will scale linearly. Since the QSO $n(z)$ is approximately independent of survey magnitude limit, the main other survey parameter is QSO sky density. We have calculated the effective volume at sky densities approximating those for the SDSS, 2QZ and 2SLAQ surveys at 10, 35 and $80\,\mathrm{deg}^{-2}$. We also present the effective volumes at $140\,\mathrm{deg}^{-2}$, which is approximately the largest density accommodated by the 2dF fibre positioner (if tiling overlaps are considered, see later), and $280\,\mathrm{deg}^{-2}$ which is the highest QSO density that is available from the Hubble Volume simulations (see Section 4.1). The assumed QSO correlation function amplitude was $s_0 = 6\,h^{-1}$ Mpc which is also found to be almost independent of survey limit (see e.g. Shanks et al. 2011). From Fig. 2 we see that QSO effective volume generally drops sharply as the spatial wavenumber increases; this drop is at a faster rate than for more highly sampled galaxy surveys such as WiggleZ.

However, even at the 2SLAQ sky density of $80\,\mathrm{deg}^{-2}$, we see that at the scale of the first acoustic peak at $k \approx 0.02\,h\,\mathrm{Mpc}^{-1}$, the effective volume of our nominal $3000\,\mathrm{deg}^2$ survey overtakes that of the current leading galaxy BAO survey, WiggleZ (Blake et al. 2011), by a factor of $\approx 3$. Of course, even if the effective
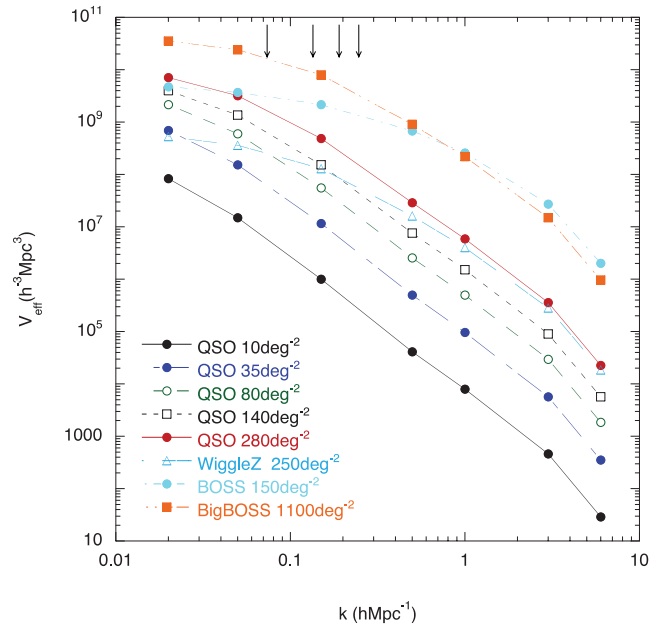


**Figure 2.** The effective volume as a function of wavenumber of spatial scale for a $z \approx 1.5$ QSO survey of area $3000\,\mathrm{deg}^2$ and QSO sky densities varying from 10 to $280\,\mathrm{deg}^{-2}$ as shown. The assumed QSO correlation function amplitude was $s_0 = 6\,h^{-1}$ Mpc. Also shown is the effective volume for the BOSS LRG survey at $z \approx 0.5$ assuming $s_0 = 10\,h^{-1}$ Mpc and $10\,000\,\mathrm{deg}^2$ area. The WiggleZ ELG survey at $z \approx 0.5$ has $s_0 = 4.4\,h^{-1}$ Mpc and $1000\,\mathrm{deg}^2$ area. The proposed BigBOSS ELG survey at $z \approx 1$ has $s_0 = 4.4\,h^{-1}$ Mpc and $14\,000\,\mathrm{deg}^2$ area. The arrows indicate the positions of the first, second, third and fourth BAO peaks (from left to right).

volume is only merely competitive with WiggleZ volume as it is at the second and third peak positions, then this still represents an advance, given the $\approx 3$ times higher redshifts of the QSOs than the WiggleZ galaxies. To reach the same effective volume at the first acoustic peak of the current BOSS LRG survey at $z \approx 0.55$, a higher QSO sky density of $140\,\mathrm{deg}^{-2}$ would be needed. This sky density would be reached at $g \approx 22.7$,[1] assuming a $10^{0.3m}$ QSO number count slope (Boyle et al. 1988). This QSO effective volume again applies at an $\approx 3$ times higher redshift than the BOSS LRGs. Even the BigBOSS Emission Line Galaxy (ELG) survey will produce an effective volume which is only $\approx 2$ times bigger than for a $140\,\mathrm{deg}^{-2}$ QSO survey when renormalized to the same area of sky. BigBOSS also has a significantly lower average redshift, $z \approx 1$. Thus, the relatively crude effective volume measure suggests that a QSO survey of nominal area $3000\,\mathrm{deg}^2$ and sky density in the range $80$–$140\,\mathrm{deg}^{-2}$ should produce large-scale clustering results that have similar precision at the first acoustic peak to the BOSS LRG survey but at significantly higher redshift.

## 4 BAO SEARCH IN SIMULATIONS

### 4.1 Hubble Volume

We next use the Hubble Volume simulation to measure the correlation function errors directly in mock surveys that range up to higher QSO sky densities than 2QZ. This simulation (Evrard et al. 2002)

---

[1] We assume that the QSO clustering and bias continue to be luminosity independent at this limit (Shanks et al. 2011).
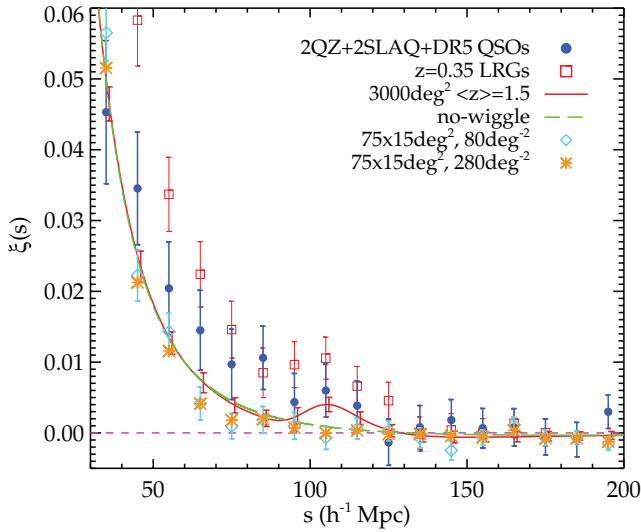
**Figure 3.** Correlation function from QSO Hubble Volume mocks at 35, 80 and 280 deg$^{-2}$ compared to $\Lambda$CDM and no-wiggle models and also the observed data. The errors found for the 80 deg$^{-2}$ case have been scaled to a 3000 deg$^2$ survey and applied to the $\Lambda$CDM model (red points + line).
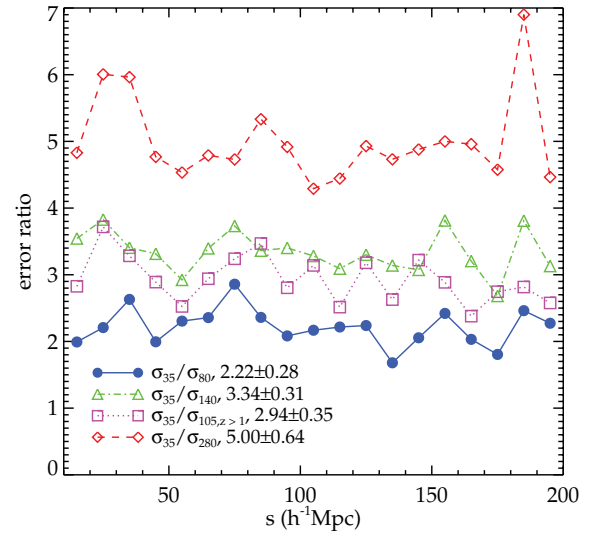


**Figure 4.** The ratio of the jack-knife errors (60 sub-samples) from the QSO mock catalogues from the Hubble Volume $N$-body simulation, using densities of 35 deg$^{-2}$, 80 deg$^{-2}$, 105 deg$^{-2}$, 140 deg$^{-2}$ and 280 deg$^{-2}$. The final ratios of $2.22 \pm 0.28$, $2.94 \pm 0.35$, $3.34 \pm 0.31$ and $5.0 \pm 0.64$ can be compared to the QSO sky density ratios of 2.29, 3.0, 4.0 and 8.0, confirming that the error scales as expected from Poisson statistics between 35 and $\approx 100$ deg$^{-2}$.

used an initial mass power spectrum with $\Omega_b = 0.04$, $\Omega_{CDM} = 0.26$, $\Omega_\Lambda = 0.7$, $H_0 = 70 \, \mathrm{km \, s^{-1} \, Mpc^{-1}}$ and $\sigma_8 = 0.9$. Mock QSO catalogues from this simulation were generated by Hoyle et al. (2002). We did consider using newer simulations but although these frequently had higher resolution, they generally did not have sufficient volume to accommodate even the original 2QZ survey. The Hubble Volume mocks are made in the form of past light cones as needed for accurate modelling of the QSO survey. The mock QSOs bias relative to the mass was modelled according to the algorithm of Hatton & Cole (1998). The main change from the previous 2QZ mocks is that the QSO sky density is approximately doubled from 35 deg$^{-2}$ to 75 deg$^{-2}$. The area of the mock survey is $15 \times 75$ deg$^2$ or 1.5 times the area of the 2QZ survey. Previously we have shown that our correlation function and power spectrum estimation techniques can accurately retrieve the input functions in real and redshift space. The errors are jack-knife estimates based on 60 sub-samples from this contiguous area. The amplitude of the correlation function at small scales is $r_0 = 6 \, h^{-1}$ Mpc, close to the $r_0 = 5.9 \, h^{-1}$ Mpc shown by the data.

Fig. 3 shows the large-scale correlation functions from the mocks with 1125 deg$^2$ area and 80 and 280 deg$^{-2}$ QSO sky densities. We find that the errors are compatible with those extrapolated using simple Poisson scaling of the data–data pairs from the 2QZ+2SLAQ survey with its smaller QSO sky density and area. In fact, we find that in the relatively small area of the Hubble Volume simulation the BAO peak is barely detected in either the mock at the standard QSO sky density of 80 deg$^{-2}$ or even at 280 deg$^{-2}$. In the $\xi(s)$ measured for the unbiased mass (not shown), the feature is detected but only at low significance, 1–2$\sigma$. Thus although no feature is detectable in the relatively small Hubble Volume mocks, these data can still be used to estimate the likely errors in the $\approx 3$ times bigger 3000 deg$^2$ nominal QSO survey considered in Section 3.

Fig. 4 shows the ratio of the jack-knife errors (60 sub-samples) from the above QSO mock catalogues from the Hubble Volume simulations. The ratio of the errors agrees with the Poisson prediction between the 35 deg$^{-2}$ and 80 deg$^{-2}$ (also 105 deg$^{-2}$ see later) sky densities but the increase to 140 deg$^{-2}$ and 280 deg$^{-2}$ only achieves

a factor of 3.3 and 5 improvement in the error rather than the Poisson predicted factor of 4 and 8, respectively. So Poisson scaling works as far as the sky density of $\approx 100$ deg$^{-2}$.

### 4.2 Lognormal simulations

We also ran static simulations similar to the Gaussian simulations of Blake & Glazebrook (2003) and Glazebrook & Blake (2005), drawing 3D mode amplitudes according to power spectra for a standard $\Lambda$CDM model. The distribution used for these realizations was updated to lognormal rather than Gaussian to mimic better the effects of non-linearities in the matter distribution (Coles & Jones 1991; Blake et al. 2011). Fig. 5(a) shows the $P(k)$ analysis of 400 simulations for a 3000 deg$^2$, $z < 2.2$ QSO survey with sky density 90 deg$^{-2}$ and a uniform space density of $n = 1.6 \times 10^{-5} \, h^3 \, \mathrm{Mpc^{-3}}$. We split the redshift range into three parts, $0.4 < z < 1.0$, $1.0 < z < 1.6$ and $1.6 < z < 2.2$ with QSO sky densities of 18, 33 and 39 deg$^{-2}$ with an infall parameter of $\beta = 0.58, 0.43, 0.32$ and $b = 1.4, 2.1, 3.0$ in successive redshift ranges (Croom et al. 2005). Although the sample is dominated by shot noise, BAOs are detectable in $P(k)$ in the second and third slices with a precision comparable to WiggleZ and SDSS LRGs. In Fig. 5(a), the dotted lines are the result of an effective volume calculation for the errors, which agrees well with the scatter in the lognormal realizations. The accuracy in the $P(k)$ BAO comes from fitting the simple Blake & Glazebrook (2003); Blake et al. (2006) model to the realizations. We detect the BAO in the $1 < z < 1.6$ bin with $\pm 5$ per cent accuracy for the BAO scale and in the $1.6 < z < 2.2$ bin with $\pm 3.7$ per cent accuracy. Overall the BAO scale accuracy in the $1 < z < 2.2$ range and $\approx 70$ deg$^{-2}$ sky density is $\pm 3$ per cent.

Fig. 5(b) shows the mean correlation function result integrated over the full $0.4 < z < 2.2$ redshift range. Again, we see the BAO feature clearly detected at $\approx 3\sigma$ relative to zero signal.
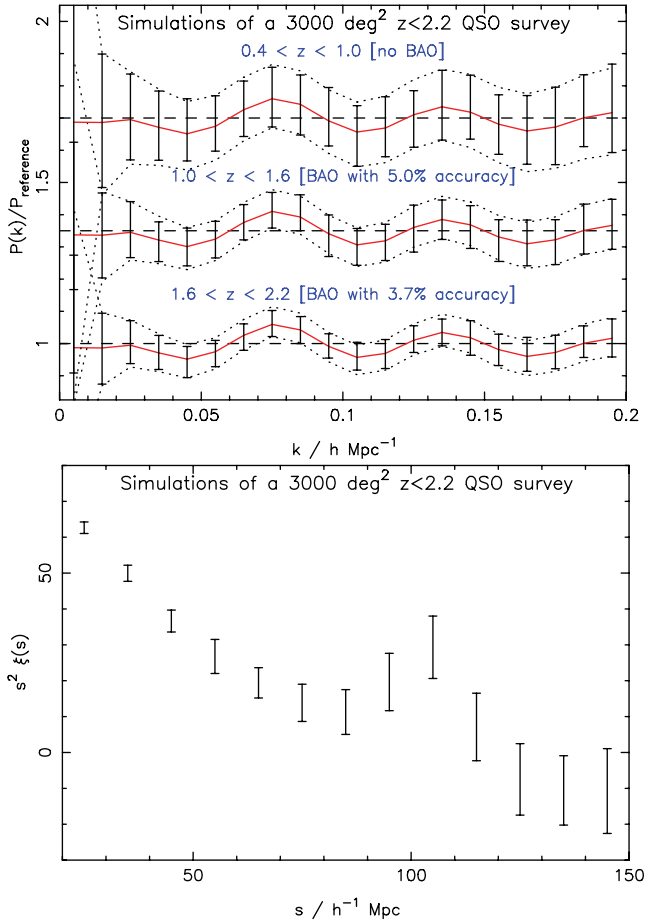
the sky density for new QSO targets might only be ≈100 deg$^{-2}$, or ≈300 per 2dF field. If these QSOs could be efficiently detected with a contamination of only 25 per cent or less then it may be possible to achieve this density with only a single 2dF pointing per field. 2SLAQ achieved a 44 per cent star contamination rate based on SDSS single epoch imaging data and improving on this rate mostly depends on achieving improved *ugriz* photometry compared to SDSS. This should be possible using new surveys such as VLT Survey Telescope (VST) ATLAS (Shanks et al., in preparation). Note also that 2SLAQ used more traditional colour cuts, and methods such as Kernel Density Estimation (KDE) (e.g. Richards et al. 2009), extreme-deconvolution, etc. would improve target selection considerably.

## 5.2 Simulated survey parameter estimates

We then take the jack-knife-based error estimates from the Hubble Volume simulation. As noted above, we have checked that the jack-knife errors reduce approximately linearly as the QSO density increases up to ≈80 deg$^{-2}$. Fig. 4 shows that as the mock QSO sky density rose from 35 to 80, 140 and then 280 deg$^{-2}$, factors of 2.3, 4 and 8.0, the jack-knife error in 60 subsamples reduced by factors of 2.22 ± 0.28, 3.34 ± 0.31 and 5.0 ± 0.64. If we drop the $z < 1$ QSOs (see below) in the 140 deg$^{-1}$ mock catalogue, the sky density becomes 105 deg$^{-1}$ and the error on the $\xi(s)$ only increases by 10 per cent. Care was taken here that the small-scale correlation function amplitude remained constant at the three sky densities so that the effect of sky density could be easily measured. These ratios also reasonably agree with taking ratios of the average of the square root of the three lowest $k$ effective volumes in Fig. 2. So we again conclude that at least up to a sky density of ≈100 deg$^{-2}$, doubling the sampling rate approximately halves the error. We also see that for the 80 deg$^{-2}$ QSO mock, extrapolating the error from the mock survey area of 1125 deg$^2$ to 3000 deg$^2$ indicates that the error is reduced to ≈27 per cent of the error in the 2QZ $\xi(s)$ results of Fig. 1, again indicating that these survey parameters will produce an ≈4$\sigma$ detection of the BAO feature in $\xi(s)$. Finally, the error on the $\xi(s)$ peak at ≈105 $h^{-1}$ Mpc in the lognormal simulations in Fig. 5(b) represents again an ≈3–4$\sigma$ detection. So there is generally excellent agreement between simulated estimates and the empirical results from Section 5.1 that a 3000 deg$^2$ QSO survey with an 80–90 deg$^{-2}$ QSO sky density will produce a significant detection of the BAO peak with a scale measurable to ≈± 3 per cent.

## 5.3 Comparison with other surveys

Fig. 6 compares the combined $1 < z < 2.2$ BAO error for the dilation scale, $D_V(z) = (D_A(z)^2 cz/H(z))^{1/3}$, of a nominal 3000 deg$^2$, 90 deg$^{-2}$ QSO survey with other current BAO surveys. The dilation scale is a measure which combines the information in the comoving angular diameter distance, $D_A(z)$, and the Hubble parameter, $H(z)$. The errors are now generated using the fitting formula of Blake et al. (2006) which is calibrated by lognormal realizations (Glazebrook & Blake 2005) for the BAO measurements. We see that the ≈± 4 per cent error from the QSO survey is comparable to the BAO error at $z = 0.35$ from the SDSS LRG survey and WiggleZ at $z = 0.6$. Note that the error derived for the dilation scale from the QSO survey-specific lognormal simulations described above is ±3 per cent which is clearly the more directly measured result. The results in Fig. 6, on the other hand, have the advantage that they are measured consistently between the various surveys.

**Figure 5.** (a) Predicted survey sensitivity for BAO from 400 lognormal simulations. Each successive set of data has been offset in *y*-axis for clarity. QSO power spectrum BAO accuracy is 3 per cent over full $1 < z < 2.2$ range in nominal survey. (b) The QSO $\xi(s)$ from the lognormal simulations integrated over the $0.4 < z < 2.2$ redshift range. The BAO signal is clearly detected.

## 5 QSO DARK ENERGY SURVEY

### 5.1 Empirical survey parameter estimates

We first take the empirical, jack-knife error estimates at 100 $h^{-1}$ Mpc from the 2QZ $\xi(s)$ result, also shown in Fig. 1. Ignoring the 2SLAQ survey simplifies the scaling of errors since in the Northern Cap at least, 2SLAQ relied on 2QZ to supply the QSOs with $b_J < 20.85$. We can then simply scale the errors from 2QZ assuming a sky density of 35 deg$^{-2}$ and an area of 750 deg$^2$. The 2QZ amplitude and error in Fig. 1 suggest that a BAO peak at ≈100 $h^{-1}$ Mpc will appear at the ≈1$\sigma$ level in a QSO sample of the current size (0.86$\sigma$ against the no-wiggle-model and 1.1$\sigma$ against zero correlation signal). Hence a ≈4$\sigma$ detection will require either a 16 times bigger survey at the 35 deg$^{-2}$ density or a four times bigger survey at double the QSO sky density. The simulation results in Fig. 4 suggest that this Poisson sky density scaling continues at least as far as ≈100 deg$^{-2}$ but not as far as 280 deg$^{-2}$. Fig. 2 also suggests that the error is 3 times rather than 4 times smaller at a QSO sky density of 140 deg$^{-2}$ compared to 35 deg$^{-2}$, so a survey of only ≈1300 deg$^2$ would be required to achieve a 4$\sigma$ BAO detection. By mainly using previous 2QZ and 2SLAQ survey areas and taking tiling overlaps of ≈20 per cent into account (to ensure survey areal completeness),
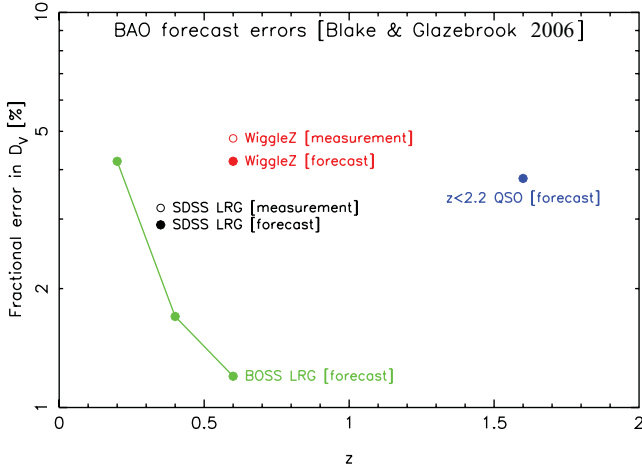
**Figure 6.** Predicted sensitivity for BAO in the nominal QSO survey consistently compared with other surveys. QSO power spectrum BAO accuracy forecasts from the fitting formula of Blake et al. (2006).

In response to a request from a referee, we note that the Hobby–Eberly Telescope Dark Energy Experiment (HETDEX) survey (Hill et al. 2008) will allow $\approx 750\,000$ Ly$\alpha$ emitting galaxies to be mapped over $1.9 < z < 3.5$ in $420\,\mathrm{deg}^2$ of sky in 150 clear nights. This survey is claimed to measure the BAO scale to $\approx 1$ per cent accuracy. This survey will therefore produce similar errors to a QSO survey with an area of $4500\,\mathrm{deg}^2$ and a sky density of $\approx 100\,\mathrm{deg}^{-2}$, in a mostly higher and hence complementary redshift range.

## 5.4 Markov Chain Monte Carlo cosmology fits

Finally, we ran some MCMC cosmology fits for *Wilkinson Microwave Anisotropy Probe* (*WMAP*) distance priors plus current and future BAO surveys for $(\Omega_\mathrm{m}, \Omega_\mathrm{m} h^2, w_0, w_a, \Omega_\mathrm{k})$ with the motivation of seeing if the data can distinguish curvature from evolving dark energy. For that reason we first focus on the joint likelihood of $(w_a, \Omega_\mathrm{k})$, which is shown in Fig. 7(a) for various combinations of surveys. We assume the CPL (Chevallier & Polarski 2001; Linder 2003) parametrization for the evolving dark energy equation of state, i.e. $w(a) = w_0 + w_a(1 - a)$. For the *WMAP* distance data we used the constraints on the shift parameter $R$, the acoustic scale $l_a$ and the redshift of recombination $z_*$, as given in Komatsu et al. (2009).

Given just SDSS-LRG + WiggleZ (not shown), our nominal $3000\,\mathrm{deg}^2/80\,\mathrm{deg}^2$ QSO survey at $z = 1.6$ does give significant help. However, Fig. 7(a) is based on *WMAP* + BOSS-LRG (+BOSS-Ly$\alpha$) and the accuracy of particularly the BOSS-LRG measurement at $z \approx 0.5$ provided by this combination means that the QSOs (green contour) will only decrease the errors in $w_a$, $\Omega_\mathrm{k}$ by at most 10–20 per cent in this parametrization. Clearly in the case where there is little evolution and $w_a \approx 0$, even in their more restricted redshift ranges, BOSS LRG and Ly$\alpha$ surveys already constrain $w_a$ as strongly as the nominal $3000\,\mathrm{deg}^2 + 80\,\mathrm{deg}^{-2}$ QSO survey at $z \approx 1.6$. The same result holds in the $w_0$, $w_a$ plane in Fig. 7(b). *On the other hand, it should be noted that the nominal QSO survey would on its own produce the first detection of, for example, discontinuous dark energy evolution in the so far unexplored $1 < z < 2.2$ redshift range.*

We next consider what survey parameters would lead to significant improvements in the cosmological forecasts, even in the case where the dark energy evolves smoothly from $z \approx 0.5$ to $z \approx 1.6$.
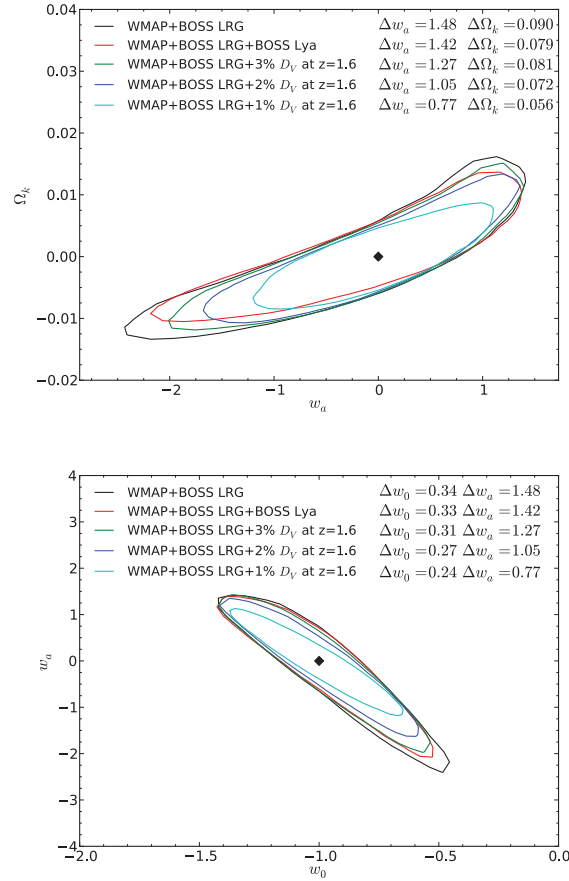


**Figure 7.** Predicted survey constraints for $\Omega_\mathrm{k}$, $w_a$, $w_0$ from BAO MCMC fits. $1\sigma$ contours and errors are shown. (a) Our nominal QSO survey produces a 3 per cent BAO error (green contour) and will provide the first detection of any non-standard (e.g. discontinuous) evolution in the dark energy equation of state in the $1 < z < 2$ range. But if the evolution remains relatively standard/continuous then a survey with a 50 per cent bigger area and a 50 per cent higher sky density will produce a 1–2 per cent QSO BAO error which will significantly improve over BOSS constraints on $w_a$ and $\Omega_\mathrm{k}$ (cyan, blue contours). (b) Similarly, even in the case of standard/continuous dark energy evolution, a survey with a 1–2 per cent BAO error will provide significantly improved constraints over BOSS in the $(w_0, w_a)$ plane (cyan, blue contours).

Bigger QSO surveys shown in Figs 7(a) and (b) assume 1 per cent and 2 per cent errors in $D_V$ and the contours suggest that a 1.5 per cent error is likely to give significantly smaller errors than the competing BOSS LRG+Lyman $\alpha$ surveys in the $w_a$, $\Omega_\mathrm{k}$ and the $w_0$, $w_a$ planes.

If so, then we would need to increase the QSO sky density by a factor of $\approx 1.6$ to $\approx 140\,\mathrm{deg}^{-2}$, reducing the QSO $D_V$ error by a factor of $\approx 1.5$ from 3 per cent to 2 per cent. This would require a 0.6 mag fainter mag limit taking us to $g < 22.5$ rather than $g < 21.85$. Then we could drop the $z < 1$ QSOs which takes us back to $\approx 105\,\mathrm{deg}^{-2}$ (see Section 5.2), without much loss of BAO S/N as evidenced from the lognormal simulations and Fig. 4. This should be possible with VST ATLAS imaging data. If we wanted to get, below a 2 per cent error then an additional $\approx 50$ per cent of the area i.e. $\approx 4500\,\mathrm{deg}^2$, would give a BAO error of 1.6 per cent. This may be possible in a 1–2 h AAOmega exposure time and the survey would then be completed in $\approx 200$ clear nights. From Fig. 7, such a QSO survey would produce an error on the dark energy evolution parameter, $w_a$, which is $\approx 60$ per cent the size of that from BOSS
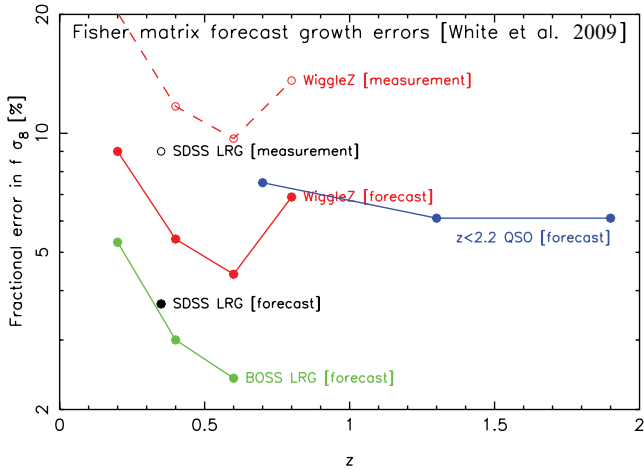
**Figure 8.** Predicted sensitivity for growth of structure in the nominal QSO survey consistently compared with other surveys. Growth of structure forecasts is generated using the Fisher matrix formula of White et al. (2009).

LRGs. The BAO detection significance would be $\approx 6\sigma$ as opposed to 3–4$\sigma$ in the nominal 3000 deg$^2$, 80 deg$^{-2}$ QSO survey.

### 5.5 Redshift-space distortions

The nominal 3000 deg$^2$ redshift survey of 250 000 QSOs would also be able to probe cosmology via redshift-space distortions. Now a redshift-space distortion test of non-Einstein gravity is more difficult at high redshift because $\Omega_m(z)$, at least in FLRW-based models, tends to unity at high $z$, making the $\gamma$ index of the gravitational growth rate (Linder 2005), $f(z) = \Omega_m(z)^\gamma$, more difficult to determine. However, interesting cosmological constraints can still be obtained. The infall parameter governing redshift-space distortions is defined as $\beta = \Omega_m^\gamma/b$, and so depends on the bias, $b$, as well as the gravitational growth rate, $\Omega_m^\gamma$. Previously for the 2QZ and 2SLAQ QSO surveys we have used redshift-space distortion and the evolution of the QSO clustering amplitude to solve for $\Omega_m(z = 0)$ and bias, $b(z = 1.6)$ simultaneously (da Ângela et al. 2005, 2008; da Ângela, Outram & Shanks 2005). This test also involves the Alcock–Pacynzski geometric test. The bias $b(z = 1.6)$ can then be used to derive the amplitude of mass clustering, i.e. $\sigma_8$, at $z = 1.4$.

Recently, the combination $f \times \sigma_8^m (= \beta \times \sigma_8^g$ if $b = \sigma_8^g/\sigma_8^m)$ has become the prime target for redshift-space distortion studies, since it can discriminate between modified gravity models without needing to determine the bias (Song & Percival 2009). Redshift-space distortions can thus provide a strong test of Einstein's gravity independently of geometrical cosmological tests that use standard candles and rods, such as BAO (Guzzo et al. 2008). Redshift-space distortions can further be used to give an estimate of the masses and hence mass-to-light ratios of galaxy group haloes in CDM models (e.g. Mountrichas et al. 2009).

In Fig. 8, we show the error in the gravitational growth rate–mass fluctuation parameter, $f\sigma_8$, for the QSO survey as estimated using the publicly available Fisher matrix code of White, Song & Percival (2009). The result is averaged over the full range of clustering scales $1 < s < 100 \, h^{-1}$ Mpc. We see that the overall result is again comparable to that for WiggleZ (Blake et al. 2011) and the SDSS LRG survey but at a significantly higher redshift. If we made a survey at the $\approx 140$ deg$^{-2}$ QSO density and over an area of 4500 deg$^2$, the error on these redshift-space distortion results would

reduce by a further factor of $\approx 1.8$ times. So with these parameters the error on $f\sigma_8$ would reduce from 6 to 3.3 per cent in this redshift range making the survey even more competitive in the $1 < z < 2.2$ range.

## 6 QSO CLUSTERING AS A PROBE OF NON-GAUSSIANITY

### 6.1 Background

Inflationary models with standard slow-roll inflation will produce very little non-Gaussianity, but models that deviate from the slow-roll assumption can produce a significantly non-Gaussian seed field (see Bartolo et al. 2004 for a review). Non-Gaussianity is normally parametrized through some amplitude of a quadratic term in the primordial Bardeen potential, $f_{NL}$. This parameter gives the coupling between a triangle of three $k$ modes, and can either be applied to the local ('squeezed' isosceles triangles) or equilateral form of non-Gaussianity. It can be measured using the large-scale galaxy Bispectrum. The best current limits on non-Gaussianity are obtained from the cosmic microwave background (CMB) radiation (Komatsu et al. 2011) which was $f_{NL}^{local} = 32 \pm 21$. Galaxy surveys can actually be more powerful as they can sample more modes in 3D space than the CMB can on the 2D surface of the sphere. It also samples the structure of matter perturbations at smaller scales, making it complementary to experiments such as *Planck*. By probing scales in the range $k = 0.01$–$0.2 \, h$ Mpc$^{-1}$, it will be able to link constraints from the CMB with constraints from clusters (LoVerde et al. 2008), constraining possible scale-dependence of the non-Gaussianity.

In galaxy surveys, non-Gaussianity can produce a scale-dependent boost of the halo power spectrum at $k < 0.03 \, h$ Mpc$^{-1}$ and this evolves as $(1 + z)$. Although this can potentially be confused with the full general relativistic correction of the galaxy power spectrum at $k \leq 0.01 \, h$ Mpc$^{-1}$, the effect becomes important only beyond $z \approx 3$ (Yoo 2010). Hence QSO surveys with their large volumes and redshift ranges make an ideal basis for this test (e.g. Slosar et al. 2008). Xia et al. (2010a,b) has recently produced upper limits on non-Gaussianity from the SDSS-DR6 photo-$z$ QSO catalogue (Richards et al. 2009) and The NRAO VLA Sky Survey (NVSS; Condon et al. 1998). The NVSS auto-correlation function shows some evidence for a positive tail extending to 5$^\circ$–6$^\circ$ (Xia et al. 2010a; confirming previous results from Blake & Wall 2002) which could be caused by non-Gaussianity, implying $f_{NL}^{local} = 62 \pm 27$. Xia et al. (2010b) found lower but still consistent angular correlation functions from a million QSOs in the SDSS DR6 data set, implying $f_{NL}^{local} = 58 \pm 24$. However, $f_{NL}$ measurements from high-$z$ photometric surveys can contain systematic bias due to gravitational lensing magnification (Namikawa, Okamura & Taruya 2011). QSO redshift surveys will provide more accurate and stringent constraints.

### 6.2 Non-Gaussianity constraints via the nominal QSO survey

A 3000 deg$^2$ QSO survey will give highly competitive constraints on primordial non-Gaussianity in the density field. Sefusatti & Komatsu (2007) calculated how effective future galaxy surveys would be at measuring the $f_{NL}$ parameters, simultaneously with the non-linear bias. Their fig. 6 shows predictions of the sensitivity of surveys of different volumes with a galaxy density of $5 \times 10^{-4} \, (h \, \text{Mpc}^{-1})^3$. Their forecasts demonstrate that our nominal QSO survey has certain advantages over its low-redshift counterparts. By

making measurements at higher redshift, it is less affected by non-linear structure formation, and can measure the Bispectrum down to smaller scales. Its main advantage will be its volume, which will be larger than most other funded surveys planned for $z > 1$. We estimate that our survey will be able to constrain $f_{NL}$ (local) with an error of about $\pm 15$, and $f_{NL}$ (equilateral) of about $\pm 150$, according to the Sefusatti & Komatsu (2007) analysis. This is better than any current survey: these authors predict uncertainties almost 10 times larger for the SDSS-LRG survey, for example. Our estimate is similar to the best current CMB result, but this would be the first competitive test made using QSOs.

### 6.3 Testing for non-Gaussianity via large-scale clustering evolution

Recently, angular correlation function studies of Extremely Red Objects (EROs) in SA22 at $z \approx 1.5$ (Kim et al. 2011) and LRGs in SDSS Stripe 82 at $z \approx 1$ (Nikoloudakis et al., in preparation) have shown evidence for a flatter slope in the range $10 < r < 100\,h^{-1}$ Mpc compared to the lower redshift, SDSS ($z \approx 0.35$), 2SLAQ ($z \approx 0.55$) and AAOmega LRG ($z \approx 0.68$) surveys. The evolution is small but statistically reasonably significant ($\approx 3\sigma$). Since evolution is not expected in the linear regime in the standard cosmological model, one interpretation of this evolution is that it might correspond to evidence for a non-Gaussian feature in the galaxy correlation function becoming more prominent at high redshifts, similar to that found above by Xia et al. (2010a) and Blake & Wall (2002).

However, the angular correlation function is particularly susceptible to artefacts in the data such as small artificial gradients. The amplitude of the redshift-space correlation function is intrinsically higher because of the lack of projection effects. Therefore, it is interesting to use the QSO clustering correlation function, $\xi(s)$, to look for evolution in the large-scale slope of the correlation function. In Fig. 9 we therefore compare the combined QSO correlation function to the 2dF Galaxy Redshift Survey (2dFGRS) $\xi(s)$ at $z \approx 0.12$ (Hawkins et al. 2003) and the SDSS LRG $\xi(s)$ at $z \approx 0.35$ (Eisenstein et al. 2005). We also show a linear model that was fitted to correlation functions from 1.5 million LRGs in three photometric samples with average redshifts $z = 0.35, 0.55, 0.68$ (Sawangwit
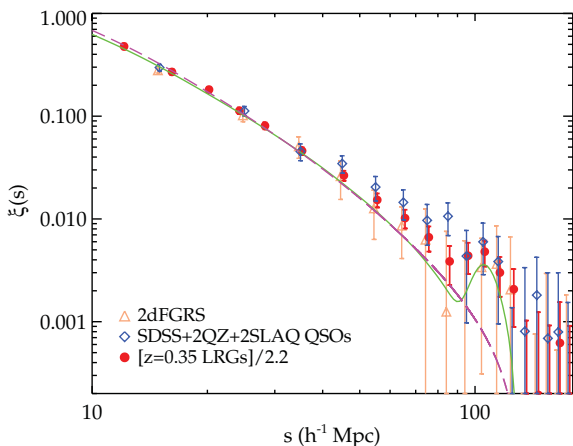
et al. 2011). This model assumes a CDM Universe with $\Omega_\Lambda = 0.73$, $\Omega_m = 0.27$, $f_{baryon} = 0.167$, $\sigma_8 = 0.8$, $h = 0.7$ and $n_s = 0.95$. This model has also been corrected for scale-dependent redshift-space distortion following Eisenstein et al. (2005). It can be seen that this model also gives an excellent fit to the 2dFGRS ($z = 0.12$) and SDSS LRG ($z = 0.35$) 3D correlation functions, $\xi(s)$, as shown. At the level of the current errors in the observed correlation functions, it is not statistically possible to distinguish the form of the observed low-$z$ galaxy and high-$z$ QSO correlation functions. However, when $\chi^2$ is fitted in the $15 < s < 95\,h^{-1}$ Mpc range, the slope of the $z \approx 1.6$ QSO correlation function appears flatter at the $2\sigma$ level than the linear model fitted to the lower redshift ($z < 0.7$) surveys.[2] This provides some limited support to the results from the LRG angular correlation functions at $z = 1$ and $z = 1.5$ but clearly more data are needed. Even the nominal QSO survey would provide an $\approx 3$–4 times reduction in the errors in the $10$–$100\,h^{-1}$ Mpc range and allow a much more significant search for non-Gaussian evolution at large QSO separations. Furthermore, the possible detection of non-Gaussian evolution in the current LRG and QSO surveys is a potent reminder that dark energy evolution at high redshift may also be of an unexpected form which should be measured rather than assumed.

## 7 OTHER QSO $z$ SURVEY SCIENCE

More QSOs will also provide new data on the small-scale amplitudes of QSO clustering as a function of luminosity and will improve $\xi(s)$ statistics at SDSS, 2QZ and 2SLAQ depths and this has importance for QSO formation and evolution models. The amplitude of QSO clustering seems remarkably independent of QSO luminosity (Shanks et al. 2011), is marginally significant (Porciani & Norberg 2006; Shen et al. 2009), and so checking for any small luminosity dependence can put strict limits on models of QSO environment and their host halo and Black Hole (BH) mass. A 3000 deg$^2$ survey will contain 30 000 QSOs at the SDSS depth, $\approx 100\,000$ at the 2QZ flux limit and $\approx 120\,000$ at the 2SLAQ limit, so there will be significant improvements in the small-scale QSO clustering measurements in all three luminosity ranges.

A further application of a QSO survey is QSO lensing via magnification bias (Myers et al. 2003, 2005; Scranton et al. 2005; Ménard et al. 2010). Myers et al. found stronger results using QSO spectroscopic $z$ than Menard et al. did using QSO photo-$z$. Mountrichas & Shanks (2007) found that contamination of the photo-$z$ QSO sample by low-redshift QSOs could reduce the anti-correlation signal that is expected from lensing of faint QSOs. A large spectroscopic QSO survey would reduce the errors on the 2QZ results significantly and test the validity of the photo-$z$ results, as well as complementing galaxy shear weak-lensing tomography.

QSO surveys also allow investigations of the topology of the Universe. For example, using the 2QZ survey, Weatherley et al. (2003) searched for exact QSO spectral pairs at large separations to check for topologically closed universes. Again a larger QSO survey would allow more stringent constraints on such models.

## 8 SUMMARY AND CONCLUSIONS

We first made a new correlation function analysis of the combined SDSS, 2QZ and 2SLAQ QSO surveys, comprising some 60 000



**Figure 9.** The combined DR5+2QZ+2SLAQ QSO correlation function from Fig. 1 now plotted on log axes and compared to the 2dFGRS $\xi(s)$ at $z = 0.12$ of Hawkins et al. and the scaled SDSS LRG $\xi(s)$ of Eisenstein et al. and a linear model fitted to LRG surveys in the range $0.35 < z < 0.7$. The slope of the QSO $\xi(s)$ at $z \approx 1.6$ is marginally ($2\sigma$) flatter than the linear model fitted at $z < 0.7$.

---

[2] Since the jack-knife errors are approximately Poisson in this range, we have ignored the covariance between points in our $\chi^2$ analysis.

QSOs. We focused on the large-scale, $s \approx 100 \, h^{-1}$ Mpc, results to test the strength of BAO signal that could be detected in the current data set. We found that the $\approx 22\,000$ 2QZ QSOs dominate the signal; although 2SLAQ has a higher sky density it has only $\approx 6000$ QSOs in total and although SDSS has a larger number of QSOs its contribution is less significant because of its low sky density. We observe a possible peak at $\approx 105 \, h^{-1}$ Mpc where the SDSS LRG $\xi(s)$ peak was found by Eisenstein et al. (2005) but here it is only detected at a low significance of $\approx 1\sigma$ in the combined data set and other peaks are seen at other separations at a similar significance.

We then proceeded to investigate the QSO survey parameters that would be needed to make an $\approx 4\sigma$ detection of the BAO peak. We conclude that our nominal survey of $250\,000$ QSOs in a sky area of $3000 \, \mathrm{deg}^2$ will allow us to make a $4\sigma$ detection of the BAO scale at $1 < z < 2.2$, an as yet unexplored range for cosmology. This $\pm 3$ per cent BAO scale measurement will determine the high-redshift evolution of the dark energy equation of state, $p = w(z)\rho$, and in particular show if there is any large ($>15$ per cent) deviation from $w = -1$ in the $1 < z < 2.2$ redshift range. But even if $w_a \approx 0$, then a survey with 50 per cent higher QSO sky density and a 50 per cent bigger area will approximately halve the BAO error to 1.6 per cent. At this point the QSO survey will also approximately halve the error on the dark energy evolution parameter, $w_a$, and significantly reduce the errors on $w_0$ and $\Omega_k$ compared to the BOSS LRG and Lyman $\alpha$ BAO results at lower and higher redshifts.

A QSO survey can also set powerful new limits on the existence of non-Gaussianity ($f_{NL}$) in the primordial density field. We have found that the combined SDSS+2QZ+2SLAQ QSO survey shows possible $\approx 2\sigma$ evidence for evolution in the linear form of the $z \approx 1.6$ QSO correlation function, in the sense that it shows a flatter slope than a linear model fitted to galaxy surveys at $z < 0.7$. Even the nominal QSO survey would improve the significance of detection of this slope change by 3–4 times. If confirmed, the result could indicate the detection of the evolution of a non-Gaussian feature in the large-scale QSO correlation function. The tentative evidence found here and in projected galaxy correlation functions for unexpected evolution of large-scale structure emphasises that dark energy evolution at high redshift may also be of an unexpected form.

The QSO survey will further support analyses of redshift-space distortions to measure $f \times \sigma_8$ and test Einstein gravity versus other modified gravity models. We shall also make the most rigorous application of the Alcock & Paczynski (1979) test so far of the prediction of the standard $\Lambda$CDM model for the amplitude of the mass clustering, $\sigma_8$, at $z \approx 1.5$. Other science it will do includes making the most accurate determination of the luminosity dependence of QSO clustering at small scales in order to probe QSO formation and evolution via QSO environment. The survey could also use QSO lensing magnification bias to measure the mass and the bias of foreground groups and clusters and to do lensing tomography.

## ACKNOWLEDGMENTS

## REFERENCES

Alcock C., Paczynski B., 1979, Nat, 281, 358
Bartolo N., Komatsu E., Matarrese S., Riotto A., 2004, Phys. Rev., 402, 103
Blake C., Glazebrook K., 2003, ApJ, 594, 665
Blake C., Wall J., 2002, MNRAS, 329, L37
Blake C., Parkinson D., Bassett B., Glazebrook K., Kunz M., Nichol R. C., 2006, MNRAS, 365, 255
Blake C. et al., 2011, MNRAS, 415, 2892
Boyle B. J., Shanks T., Peterson B. A., 1988, MNRAS, 235, 935
Chevallier M., Polarski D., 2001, Int. J. of Modern Phys. D, 10, 213
Coles P., Jones B., 1991, MNRAS, 248, 1
Condon J. J., Cotton W. D., Greisen E. W., Yin Q. F., Perley R. A., Taylor G. B., Broderick J. J., 1998, AJ, 115, 1693
Croom S. M., Smith R. J., Boyle B. J., Shanks T., Miller L., Outram P. J., Loaring N. S., 2004, MNRAS, 349, 1397
Croom S. M. et al., 2005, MNRAS, 356, 415
Croom S. M. et al., 2009, MNRAS, 399, 1755
da Ângela J., Outram P. J., Shanks T., Boyle B. J., Croom S. M., Loaring N. S., Miller L., Smith R. J., 2005, MNRAS, 360, 1040
da Ângela J., Outram P. J., Shanks T., 2005, MNRAS, 361, 879
da Ângela J. et al., 2008, MNRAS, 383, 565
Eisenstein D. J., Hu W., 1998, ApJ, 496, 605
Eisenstein D. J. et al., 2005, ApJ, 633, 560
Evrard A. E. et al., 2002, ApJ, 573, 7
Glazebrook K., Blake C., 2005, ApJ, 631, 1
Guzzo L. et al., 2008, Nat, 451, 541
Hamilton A. J. S., 1993, ApJ, 417, 19
Hatton S., Cole S., 1998, MNRAS, 296, 10
Hawkins E. et al., 2003, MNRAS, 346, 78
Hill G. J. et al., 2008, in Kodama T., Yamada T., Aoki K., eds, ASP Conf. Ser. 399, Panoramic Views of Galaxy Formation and Evolution. Astron. Soc. Pac., San Francisco, p. 115
Hoyle F., Outram P. J., Shanks T., Boyle B. J., Croom S. M., Smith R. J., 2002, MNRAS, 332, 311
Kim J.-W., Edge A. C., Wake D. A., Stott J. P., 2011, MNRAS, 410, 241
Komatsu E. et al., 2009, ApJS, 180, 330
Komatsu E. et al., 2011, ApJS, 192, 18
Landy S. D., Szalay A. S., 1993, ApJ, 412, 64
Lewis I. et al., 2002, MNRAS, 334, 673
Linder E. V., 2003, Phys. Rev. L., 90, 091301
Linder E. V., 2005, Phys. Rev. D., 72, 043529
LoVerde M., Miller A., Shandera S., Verde L., 2008, J. Cosmol. Astropart. Phys., 0804, 014
Ménard B., Scranton R., Fukugita M., Richards G., 2010, MNRAS, 405, 1025
Mountrichas G., Shanks T., 2007, MNRAS, 380, 113
Mountrichas G., Sawangwit U., Shanks T., Croom S. M., Schneider D. P., Myers A. D., Pimbblet K., 2009, MNRAS, 394, 2050
Myers A. D., Outram P. J., Shanks T., Boyle B. J., Croom S. M., Loaring N. S., Miller L., Smith R. J., 2003, MNRAS, 342, 467
Myers A. D., Outram P. J., Shanks T., Boyle B. J., Croom S. M., Loaring N. S., Miller L., Smith R. J., 2005, MNRAS, 359, 741

Namikawa T., Okamura T., Taruya A., 2011, Phys. Rev. D, 83, 123514

Osmer P. S., 1981, ApJ, 247, 762

Outram P. J., Hoyle F., Shanks T., Croom S. M., Boyle B. J., Miller L., Smith R. J., Myers A. D., 2003, MNRAS, 342, 483

Porciani C., Norberg P., 2006, MNRAS, 371, 1824

Richards G. T. et al., 2009, ApJS, 180, 67

Ross N. P. et al., 2009, ApJ, 697, 1634

Sawangwit U., Shanks T., Abdalla F. B., Cannon R. D., Croom S. M., Edge A. C., Ross N. P., Wake D. A., 2011, MNRAS, 416, 3033

Schneider D. P. et al., 2007, AJ, 134, 102

Scranton R. et al., 2005, ApJ, 633, 589

Sefusatti E., Komatsu E., 2007, Phys. Rev. D, 76, 083004

Shanks T., Croom S. M., Fine S., Ross N. P., Sawangwit U., 2011, MNRAS, 416, 650

Shen Y. et al., 2009, ApJ, 697, 1656

Slosar A., Hirata C., Seljak U., Ho S., Padmanabhan N., 2008, J. Cosmol. Astropart. Phys., 08, 031

Smith G. A. et al., 2004, SPIE, 5492, 410

Song Y.-S., Percival W. J., 2009, J. Cosmol. Astropart. Phys., 10, 4

Wang X., Chen X., Zheng Z., Wu F., Zhang P., Zhao Y., 2009, MNRAS, 394, 1775

Weatherley S. J., Warren S. J., Croom S. M., Smith R. J., Boyle B. J., Shanks T., Miller L., Baltovic M. P., 2003, MNRAS, 342, L9

White M., Song Y.-S., Percival W. J., 2009, MNRAS, 397, 1348

Xia J.-Q., Viel M., Baccigalupi C., De Zotti G., Matarrese S., Verde L., 2010a, ApJ, 717, L17

Xia J.-Q., Bonaldi A., Baccigalupi C., De Zotti G., Matarrese S., Verde L., Viel M., 2010b, J. Cosmol. Astropart. Phys., 8, 13

Yoo J., 2010, Phys. Rev. D, 82, 083508

This paper has been typeset from a TEX/LATEX file prepared by the author.